

Ionization Energy of CF_3 Deduced from Photoionization of Jet-Cooled CF_3Br

Gustavo A. Garcia

School of Chemistry, University of Nottingham, Nottingham NG7 2RD, UK

Paul-Marie Guyon

L.C.A.M., Université Paris Sud, 91405 Orsay, France

Ivan Powis*

School of Chemistry, University of Nottingham, Nottingham NG7 2RD, UK

Received: March 16, 2001; In Final Form: June 25, 2001

The ionization energy of CF_3^+ is investigated by synchrotron radiation photoionization experiments using a skimmed molecular beam of CF_3Br . Care is taken to eliminate contributions from higher energy second-order radiation from the monochromator gratings and to characterize the molecular beam. From the corrected 0 K CF_3^+ appearance energy of 12.07 ± 0.02 eV, we calculate the adiabatic CF_3 ionization energy to be 9.04 ± 0.04 eV, a value in excellent agreement with recent calculations and a number of experiments. Apparent discrepancies with other, significantly lower, determinations of the ionization potential are discussed and explained – particularly those arising from a previous CF_3Br molecular beam experiment – confirming a recently proclaimed consensus favoring a value as obtained here.

I. Introduction

The CF_3 radical and its cation are of undoubted importance in technological processes such as plasma etching and in the environmental degradation of released refrigerants, flame inhibitors, and so on. Yet while lingering uncertainties regarding the neutral's enthalpy (and those of many CF_3X precursor species) may have recently been resolved,¹ there persists a surprisingly wide variation in the reported adiabatic ionization energy (IE) of the free radical.

In Table 1, we reproduce selected values quoted for this ionization energy. While the earliest value² of 9.25 ± 0.04 is generally recognized to be too high, other determinations span from 8.6 to ~ 9.1 eV, tending to polarize at the extremes of this range. A critical review and discussion of much of the earlier experimental data can be found in the article by Asher and Ruscic.³ Further discussion can be found in the work of Jarvis and Tuckett⁴ and most recently that of Irikura.⁵ The reader is referred to the introductions of these three papers for a more extensive discussion than attempted here.

The fundamental difficulty for experimental determinations is the extensive geometry change from pyramidal CF_3 to planar CF_3^+ . Consequently the Franck–Condon factors for the adiabatic ionization are negligible, rendering it effectively impossible to observe directly the adiabatic ionization threshold. Indeed, it has been calculated that the vertical ionization is to $\nu_2^+ = 20$ of the cation.⁶ Consequently, there is a need to resort to indirect measurements. One such approach is the determination of CF_3^+ fragment appearance energies (AEs) from ionization of a suitable precursor. A thermodynamic cycle then yields an estimate for $\Delta H_f(\text{CF}_3^+)$ from which, assuming a value for $\Delta H_f(\text{CF}_3)$, the ionization potential (IP) of CF_3 can be deduced.

However, as pointed out by Asher and Ruscic,³ a problem afflicting this general approach has been an inconsistency between authors in the methods applied to correct for thermal

TABLE 1: Some Selected Literature Values for the Ionization Potential of CF_3^+

IP (eV)	methods ^a	ref
9.25 ± 0.04	PI $\text{CF}_3^+/\text{CF}_3$	2
9.17 ± 0.08	AEs CF^+ , $\text{CF}_3^+/\text{C}_2\text{F}_4$	8
9.05 ± 0.02	as above, with revised IP(CF)	8,9
$\geq 9.055 \pm 0.011$	AEs CF^+ , $\text{CF}_3^+/\text{C}_2\text{F}_4$	3
$\leq 8.8 \pm 0.2$	AE $\text{CF}_3/\text{C}_3\text{F}_8$	4
8.69 ± 0.13	ion–molecule reaction data	4,10,11
8.60 ± 0.06	AE $\text{CF}_3^+/\text{CF}_3\text{Br}$	7
9.04 ± 0.04	AE $\text{CF}_3^+/\text{CF}_3\text{Br}$	present work
Ab Initio Calculated Values		
8.98 ± 0.05		6
9.08		1
9.10 ± 0.05		12
9.09		13
9.061		14

^a PIMS: photoionization mass spectrometry. AE: fragment appearance energy. IP: ionization potential.

energy and so extrapolate to the 0 K values. This then introduces uncertainty into the values estimated for $\Delta H_{f0}(\text{CF}_3^+)$ and hence for the adiabatic IE. Using a carefully defined extrapolation procedure themselves, these authors¹⁵ deduce what is probably the most precise experimental estimate to date for $\text{IP}(\text{CF}_3) \geq 9.055 \pm 0.011$ eV from the difference in AE of fragments CF^+ and CF_3^+ from C_2F_4 . Nevertheless, this analysis hinges on the proposition that there is no difference in kinetic shift between the two fragment channels,^{3–5} which is not a priori self-evidently the case, so that further corroboration is desirable.

Strong support does indeed come from recent ab initio calculations, summarized here in Table 1. The four latest values which have been computed or inferred are in close agreement with the above experimental value and Botschwina's group have very recently stated that their earlier, lower result (8.98 eV⁶) should be considered to have been superseded by a revised¹⁴ value of 9.061 eV. But this cluster of IP values between 9 and

TABLE 2: Photoionization Appearance Energies for CF₃⁺/CF₃Br

AE (eV)	temp. (K)	ref.
11.92 ± 0.02	300	16
11.56 ± 0.02	30	7
12.095 ± 0.005	0 (extrap.)	3
12.07 ± 0.02	0 (extrap.)	present work

9.1 eV is at variance with other, lower experimental determinations listed in Table 1. Some of these data, those derived from ion–molecule reaction data, have been reexamined by Irikura,⁵ who proposes that they also may be revised upward by recognition of, and allowance for, entropic effects.

The most significant remaining low value, 8.60 ± 0.06 eV, is inferred from the work of Clay et al.,⁷ who examined the threshold for production of CF₃⁺ in a cooled supersonic beam of CF₃Br. Because of the low temperature achieved (~30 K), much of the uncertainty associated with thermal contributions to observed appearance thresholds is avoided by making, effectively, direct observation of the near 0 K AE threshold. The need for an extrapolation to estimate the 0 K limit is thus largely obviated. But these authors report a very much lower AE than do others^{3,16} examining the same system (see Table 2), lower even than previous room-temperature thresholds. Their data takes the form of a long low-intensity tail extending down to an observed onset of 11.56 eV. It has been suggested that the superior sensitivity obtained in this synchrotron radiation-based experiment may explain the first observation of this extended weak tail. However, as seen in Table 1 the low value for IP (CF₃) deduced in consequence is increasingly looking to be at odds with most other estimations.

We here present a new investigation of the jet-cooled CF₃⁺/CF₃Br system carried out in an attempt to resolve the seeming contradictions between the low IP(CF₃) deduced from the analogous study of Clay et al.⁷ and the emerging consensus in favor of a higher value of ~9.05 eV. Both the synchrotron and molecular beam sources employed were carefully characterized in this study. Contamination of the photon source by higher energy second-order grating light was eliminated by features of experimental design and method, while the temperatures actually attained in the cooled molecular beam were examined and careful allowance for these made in the data analysis in order to obtain a reliable 0 K appearance energy for CF₃⁺.

II. Experimental Details

Experiments were performed using the SAPHIRS molecular beam spectrometer¹⁷ on two beamlines at the Super-ACO synchrotron (LURE). On the SA63 bending magnet beamline, for measurements made below a photon energy of 12.5 eV the 3-m normal incidence monochromator was equipped with a 2000 l/mm grating blazed at 1200 Å, while at higher energies a 1800 l/mm grating blazed at 820 Å was used. For measurements made on the SU5 undulator beamline,¹⁸ its 6.65-m Eagle off-plane normal incidence monochromator was used with 2400 l/mm grating blazed at 900 Å. This beamline is also equipped with a gas harmonic filter¹⁹ which, used with Ar, effectively removes second- and higher order radiation from the delivered ~12 eV photon beam with an attenuation factor > 10⁵.

On either beamline, the monochromator slits were adjusted to obtain a typical photon bandwidth ≈3–5 meV. Photon beam intensity was monitored using a fluorescent screen/photomultiplier or a gold wire grid. All data presented below were thus normalized against any variations in photon flux. The wavelength calibration of the SU5 beamline has recently been

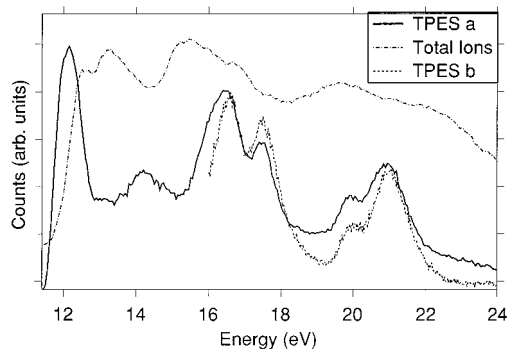


Figure 1. CF₃Br TPES. The solid curve (a) was obtained in this work. The broken curve (b) (not previously published) was obtained by Creasey et al. in pursuance of earlier studies.¹⁶ Also included is the total ion yield curve.

extensively described,¹⁸ while that of the SA63 beamline was similarly checked by recording rare gas thresholds.

A commercial mixture of 10% CF₃Br in He was expanded through a 75-μm nozzle from a backing pressure of 1.4 bar. The skimmed molecular beam enters the ionization chamber, at a pressure ≤10⁻⁶ mbar, where it is intersected by the synchrotron radiation beam. While on SA63 the linearly polarized light was parallel to the molecular beam, on SU5 the polarization was set to be linear but parallel to the TOF axis (perpendicular to molecular beam). However, no consequences of these differing polarization geometries were noted in comparisons of the near-threshold data presented here.

Ions and electrons produced are extracted, at right angles to the molecular and photon beams, into a double time-of-flight spectrometer previously described.²⁰ The photoelectrons are accelerated toward the electron detector by a constant weak electrostatic field; on arrival they trigger a positive repeller pulse to extract the ions from the source region and direct them through a second acceleration region to a drift region before they strike a multichannel plate ion detector. In multipacket operation of the S-ACO storage ring, near to threshold electrons are selected by steradiancy analysis, while in the four bunch operation mode, the interpulse gap of 120 ns is sufficient to permit electron TOF analysis referenced from the S-ACO timing signal; in either case, the ion TOF is measured against the electron signal. The electronics can be set to operate in uncorrelated mode, allowing us to look at electrons and ions separately, or in electron–ion coincidence mode suitable to study fragmentation from energy-selected states of the parent ion CF₃Br⁺.

III. Results

A modest resolution threshold photoelectron spectrum (TPES) recorded with steradiancy electron analysis (hence with some residual contribution from “hot” electrons) and step increments of 0.05 eV is shown in Figure 1. The TPES shows the main bands identified as the \tilde{X} to \tilde{F} ionic states and is essentially identical to both an earlier TPES¹⁶ and He I, He II PES.²¹ The expected spin–orbit splitting of the ground-state ion (~0.3 eV) is not resolved in any of these spectra. Surprisingly, we see no evidence of the 23.7 eV band observed in the He II spectrum,²¹ but comparison with a previously unpublished TPES obtained at 0.02 eV resolution during an earlier investigation of CF₃Br¹⁶ confirms this observation.

We have very carefully examined the ion mass spectrum in the 11.5–11.8 eV region making measurements at a number of discrete wavelengths (0.05 eV intervals) in this range. Although

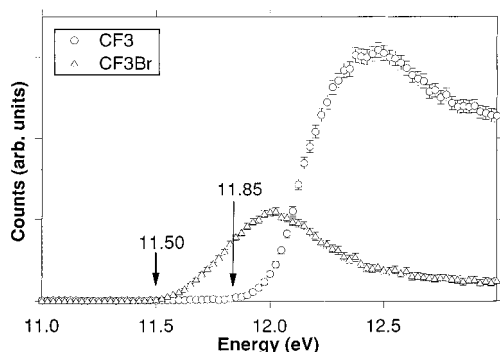


Figure 2. Near-threshold photoion yield curves for CF_3Br^+ and CF_3^+ . Experimental error bars are shown unless they would be less than the diameter of the plotting symbol. Arrows are drawn to indicate the first statistically significant rise above the baseline in the threshold regions.

traces of CF_3^+ ion could be detected, they were completely removed following the insertion of a LiF window into the monochromatized synchrotron radiation beam, indicating that the only source of CF_3^+ in our experiments at these low photon energies stemmed from contamination by second-order grating light.

Unfortunately, the LiF transmission cutoff at ~ 11.8 eV overlaps the upper end of the CF_3^+ threshold region of interest here, so that to eliminate any effects of second-order light contamination throughout the full range of interest, alternative strategies have to be adopted. Our principal tactic was to record electron-ion coincidences using a continuous dc source extraction field and steradiance analysis to select just near-threshold energy electrons. Detection of these electrons was used to start timing the ion TOF, yielding coincidence mode mass spectra. Having above established that, by serendipity, there are no near-threshold energy electrons produced at $h\nu \approx 24$ eV, this coincidence mode detection scheme effectively discriminates against any ions produced by second-order radiation transmitted with the monochromator set in first order for $h\nu \approx 12$ eV.

In Figure 2, we present such coincidence mode mass-resolved CF_3Br^+ and CF_3^+ photoion yield curves recorded in the near-threshold region obtained using beamline SA63 and the 2000 l/mm grating. (Because only low electron energy resolution is employed, we refrain from describing these as full TPEPICO measurements.) Taking, for the moment, threshold energies to be defined as the point at which the signals first exceed the background by a statistically significant amount, we obtain IP- $(\text{CF}_3\text{Br}) = 11.50 \pm 0.03$ eV, which is intermediate between earlier values of Clay et al.⁷ (11.40 ± 0.01 eV) and Creasey et al.¹⁶ (11.63 ± 0.05 eV). However, we will caution below that the lower estimates, obtained with molecular beam sources, may not reliably represent the monomer CF_3Br adiabatic ionization potential.

Similarly, from the first observed onset of the CF_3^+ photoion yield curve (Figure 2), we can obtain a first estimate of the threshold appearance energy for $\text{CF}_3^+/\text{CF}_3\text{Br}$ of 11.85 ± 0.03 eV. This is very significantly different from the AE of 11.56 ± 0.02 eV reported by Clay et al.⁷ in a closely analogous molecular beam experiment (who also used the same procedure to define an experimental onset), and so calls for further examination of the discrepancy in the data sets and, indeed, of the relationship of such “first onset” estimates from a molecular beam source to the true 0 K threshold.

The coincidence mode ion yield data of Figure 2 may also be presented in the form of a breakdown diagram, Figure 3. Although the 50% crossover observed at 12.09 eV may be interpreted²² as an approximate indication of the $\text{CF}_3^+/\text{CF}_3\text{Br}$

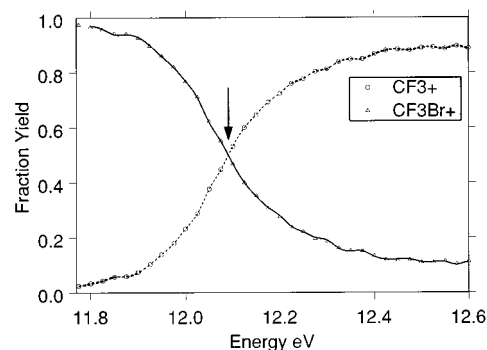


Figure 3. Breakdown diagram prepared from mass selected ion yield data. The 50% crossover point at 12.09 eV is arrowed.

appearance threshold, it is shifted by any thermal internal energy content of the parent ion and convoluted by the instrument function. In fact, using only steradiance electron analysis with a static drawout field as was done here, the electron transmission function has a long tail to high energy, extending some 0.5 eV or more, so that the instrument function applying to Figure 2 is both broad and asymmetrically tailed to low ionization energy. This determination cannot, then, be considered precise.

In the Clay experiments, the molecular beam rotational temperature was stated to be 30 K; the nozzle expansion conditions employed for our experiments can achieve a lower translational temperature of 10 K, as measured by the width of Ar^+ TOF peaks. This difference is unlikely to account for the discrepancy in the CF_3^+ onset thresholds. Both quoted beam temperatures are so low that one might assume, as did Clay et al.,⁷ that the observed onsets closely correspond to the adiabatic 0 K fragment appearance threshold. This interpretation presupposes that the molecular beam expansion is comparably effective in cooling vibrations, but this is unlikely to be a good assumption. Given that the reliability of the methodology for identifying the onset by visual examination of the data is also open to criticism,³ we have opted to apply the more detailed extrapolation procedures proposed by Asher and Ruscic.^{3,15}

Their method takes into account the form of the internal energy probability distribution, $P(E)$, by convoluting the latter with a parametrized extrapolation, or kernel, function $f(E)$:

$$f(E) = A[1 - \exp\{-B(E - E_0)\}] \quad E > E_0 \quad (1)$$

$$= 0 \quad E < E_0 \quad (2)$$

where E_0 is the 0 K threshold energy. Thus, the final model function takes the form:

$$I(h\nu) = \int_{\epsilon_0}^{\infty} P(\epsilon - h\nu)f(\epsilon)d\epsilon \quad (3)$$

with $\epsilon_0 = E_0$ if $h\nu < E_0$ and $\epsilon_0 = h\nu$ if $h\nu > E_0$.

Unlike the purely wavelength-dependent photoion efficiency (PIE) curves which Asher and Ruscic had in mind, the present ion yield data also have some additional energy selection due to the coincidence recording mode. However, as explained above, the ion energy resolution resulting from the steradiance electron analysis is only modest. Consequently, our data more closely resemble moderately differentiated P. I. E. curves than fully energy-selected, high-resolution TPEPICO curves. (This can be verified by direct comparison with the form of the fully integral CF_3Br PIE curves reported by Asher and Ruscic.³) Now since the proposed PIE kernel function (eq 1) is not based upon physical arguments, but rather is justified by its flexibility to

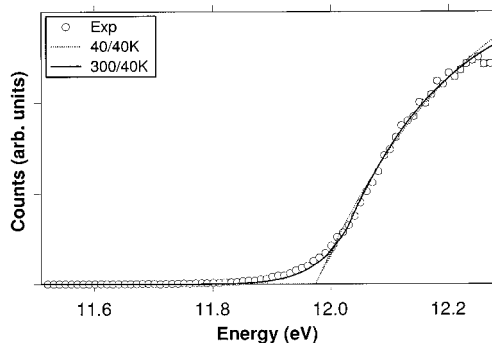


Figure 4. Expanded view of CF₃⁺ threshold region around $h\nu \approx 12$ eV recorded at 10 meV intervals on the SU5 beamline. Experimental error bars are largely obscured as they are mostly less than the diameter of the plotting symbols. Fitted extrapolation functions, eq 3, obtained with the internal energy distribution, $P(E)$, evaluated at fixed vibrational-(rotational) temperatures of 40 K (40 K) and 300 K (40 K) are included.

fit the observed data, its adoption here may be equally pragmatically justified.

The parent internal energy distribution in the molecular beam, $P(E)$, was calculated by direct counting over rotational and vibrational states weighted by a thermal Boltzmann distribution for respective temperatures T_{rot} and T_{vib} . Equation 3 could then be fitted to the experimental ion yield data, allowing only the A , B , and E_0 parameters to change. Figure 4 shows a result obtained using an assumption that $T_{\text{rot}} = T_{\text{vib}} = 40$ K internal temperature in the beam. While the kernel function fits well to the rising experimental ionization yield above ~ 12.1 eV, the convolution with the 40 K $P(E)$ fails to reproduce the observed spread of the foot of the curve to below 12 eV.

This has been further investigated by a variety of fits in which the temperature parameters could also be floated and using a number of experimental data sets including one recorded on beamline SU5 with its gas harmonic filter ensuring complete rejection of any grating orders above the desired first order $h\nu \approx 12$ eV. This latter also benefits from improved signal due to the higher photon flux from the undulator. Very consistent results were obtained in all cases, with the estimated threshold E_0 not, in fact, proving to be very sensitive to assumed temperature.

A best fit obtained with T_{rot} fixed at 40 K and T_{vib} fixed at 300 K is also shown in Figure 4. The overall quality of the fit now suggests that the indicated extrapolation to $AE_{0K} = 12.07 \pm 0.02$ eV could be simply accepted, but while the relative magnitudes of the effective translational, rotational, and vibrational beam temperatures are in the order expected from the likely efficiency of cooling of these degrees of freedom in a supersonic beam, the apparent lack of *any* vibrational cooling may nevertheless seem surprising.

Insight may be gained by examining TPEPICO CF₃Br⁺ TOF peaks obtained in the CF₃⁺ threshold region. Figure 5 shows a typical example recorded at 11.7 eV photon energy. The same parent ion TOF peak shape was seen at different photon energies along the onset region: two narrow peaks which correspond to the two isotopomers CF₃⁷⁹Br and CF₃⁸¹Br at natural atom abundance, and with an intrinsic width corresponding to the expected low translational beam temperature of 10 K, superimposed on a broader pedestal, whose width is essentially that expected for thermal 300 K CF₃Br⁺. The estimated number density of CF₃Br in the beam (≈ 0.03 mbar) exceeds that of background CF₃Br (inferred from the observed 3×10^{-7} mbar increase in chamber pressure during experiments) by many orders of magnitude, so that even allowing for differing effective

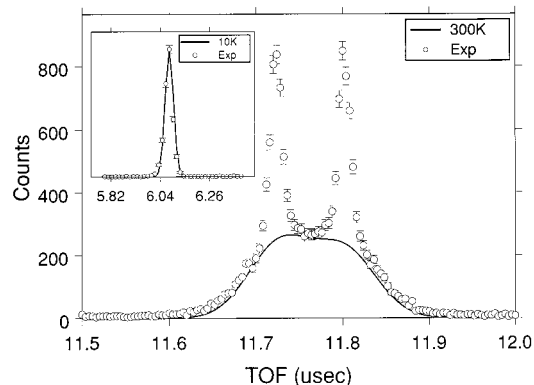


Figure 5. CF₃Br⁺ TPEPICO TOF peak, $h\nu = 11.7$ eV, showing the ⁷⁹Br and ⁸¹Br isotope splitting. A simulated 300 K thermal CF₃Br⁺ shape is included for comparison. The inset shows an analogous Ar⁺ TOF peak which is well reproduced by a simulation with just the 10 K effective translational temperature expected in the supersonic beam.

ionization volumes for background and beam gas and so on, it is unlikely that this thermal pedestal could arise simply from ionization of scattered background gas in the chamber.

It was found that the relative intensity of the pedestal could be increased by misaligning the nozzle–skimmer geometry, presumably thereby preventing skimming of just the coldest central core region of the supersonic expansion, but we were unable to reduce it to below an estimated 25% contribution. While it is possible that this may indicate some residual spoiling of the beam by nozzle–skimmer interaction, with a consequent heating of CF₃Br in the outer region of the beam, there is no indication of such an undesired thermal pedestal or spoiling in Ar⁺ TOF peak shapes measured under similar expansion conditions (see Figure 5 inset). It is then also possible that the residual translationally hot CF₃Br in the beam arises somehow from “slippage” of the heavier molecules in the seeded expansion, with a reduction in the efficiency of their cooling.

But such partially broadened peak shapes are also known to result from the release of energy following fragmentation to the monomer by dimer and higher cluster species on their ionization.²³ While no direct observation of dimer species was made in the present experiments, dimers and higher clusters have been reported⁷ in supersonic CF₃Br beams seeded in Ar. The possible involvement of cluster species may be explored by modeling the observed CF₃Br TOF peak shapes to deduce the distribution of translational energy.^{20,24,25} In so doing, we simultaneously fit the peak with two Gaussian functions—approximating the expected contributions from ionization of the two isotopomer monomer species, each having a width corresponding to a 10 K beam translational temperature—plus a broader velocity distribution, assumed to result from cluster fragmentation. To apply correct treatment for the spread of flight times attributable to the statistical distribution of isotope masses in the clusters, and to convert the speed distribution to a center of mass (CM) energy, we assume the dominant cluster contribution is from the dimer species. The results of this fitting are shown in Figure 6 together with the presumed CM kinetic energy distribution (KERD) corresponding to the TOF pedestal.

Relatively little is known about the CF₃Br dimer, but the neutral binding energy has been estimated with the aid of a rudimentary calculation²⁶ to be ~ 3 kJ mol⁻¹ (≈ 0.03 eV), that of the dimer ion (assuming it to contain a well-defined CF₃Br⁺ moiety viz. CF₃Br·CF₃Br⁺ ~ 15 kJ mol⁻¹ (≈ 0.16 eV)). These different interaction strengths may be expected to result in different equilibrium van der Waals bond lengths for the neutral and ion dimers, with a further consequence being that in the

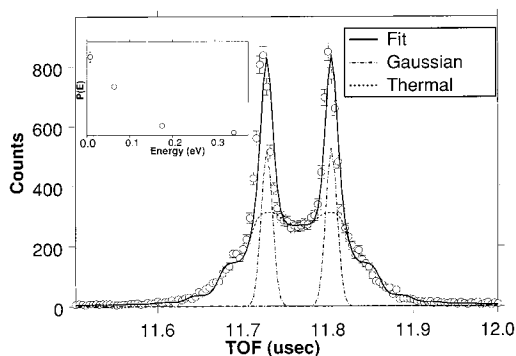
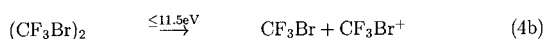
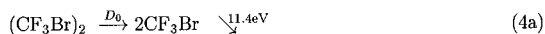


Figure 6. $h\nu = 11.7$ eV CF_3Br^+ TPEPICO TOF peak (as in Figure 5), fitted (solid curve) assuming some contribution from dissociated dimer ion species. Also shown is the decomposition of the overall fit into (a) two narrow (10 K) Gaussian peaks corresponding to the expected two isotopomer parent ions and (b) the broader pedestal contributed by quasi-thermal CF_3Br^+ ; i.e. those postulated to have originated from cluster ions. The inset panel shows the KERD so deduced.

vertical Franck–Condon excitation region the dimer ion is probably effectively unbound. One thus infers a possible lack of stability of the CF_3Br dimer with respect to its ionization. This would be consistent with our non-observation of this species, with the further assumption that the dimer cations observed by Clay et al.⁷ may in fact have resulted from dissociative ionization of even larger clusters whose formation was enhanced by the different expansion conditions employed. A similar lack of cluster ion stability has been found previously, for example²⁷ in the polar molecule dimer $(\text{C}_2\text{H}_5\text{Cl})_2$.

The mean CM energy of the distribution plotted in Figure 6 is $\langle E \rangle = 0.11 \pm 0.01$ eV, but the distribution extends to above 0.2 eV. Since the photon energy here is 11.7 eV, this energy release would fix an upper limit on the adiabatic appearance energy of CF_3Br^+ from its dimer; hence, $\text{AE}_{0\text{K}}(\text{CF}_3\text{Br}^+ / (\text{CF}_3\text{Br})_2) \leq 11.5$ eV. Taking for the moment $\text{IP}(\text{CF}_3\text{Br}) = 11.4$ eV,⁷ we may infer the binding energy of the neutral dimer ≤ 0.1 eV. Similarly taking $\text{IP}((\text{CF}_3\text{Br})_2) = 11.1$ eV⁷ suggests a $(\text{CF}_3\text{Br})_2$



Br_2^+ dimer binding energy ≤ 0.4 eV. While the associated errors are admittedly large, these estimates of binding energy are quite consistent with the theoretical estimates.²⁶

IV. Discussion

These results may serve to highlight a general danger in presuming that the observed fragment onset in a jet-cooled experiment approximates well to the 0 K appearance energy. It is already well established that vibrational cooling in supersonic beams may be inefficient, and that the vibrational temperatures achieved may significantly lag the rotational and translational temperatures. In the present case, it is also demonstrated that both cold and (quasi-)thermal translation populations may be simultaneously present in the parent ions created by photoionization. While it is not possible to unambiguously identify the mechanism that results in such a two-component translational distribution, each candidate considered may have the same consequences for internal molecular excitation. If the presence of the thermal translational component is in some way inherent to the beam expansion conditions established, it seems entirely

plausible that there would be concomitant reductions in the parent molecule vibrational cooling efficiency.

On the other hand, it is at least feasible that dissociating dimer species may play some role in such photoionization measurements. Here, in the region close to threshold for CF_3^+ formation, if some of the released cluster binding energy were to be partitioned into internal degrees of freedom in the dissociating van der Waals dimer, then that part residing in the CF_3Br^+ , at least, could facilitate the further dissociation to produce CF_3^+ . In other words, the effective CF_3Br^+ energy available to drive its fragmentation below the 0 K threshold could be expected to be enhanced when the CF_3Br^+ results from dimer ionization.

In all cases, therefore, the application of a well-defined extrapolation procedure seems to have merit for the reliable identification of the 0 K onset. There remains, of course some question as to whether this observed threshold corresponds to the true adiabatic threshold, but at the very least, there is some consistency in this data treatment.^{3,5} Here, we find the extrapolation from the ion yield curve above the threshold provides quite consistent $\text{AE}_{0\text{K}}$ estimates. But one's overall confidence in the procedure is, of course, improved by obtaining a good model fit for the "thermal" tail which can also be made physically plausible, as we have sought to do here.

Taking our optimized value of $\text{AE}_{0\text{K}} = 12.07 \pm 0.02$ eV, the most direct way to obtain independent estimates of $\text{IP}(\text{CF}_3)$ makes use of reported $\text{CF}_3\text{--Br}$ bond dissociation energies; appropriate 0 K values are²⁸ 69.8 ± 1.0 kcal mol⁻¹ or 70.8 ± 0.2 kcal mol⁻¹.^{29,30} These give $\text{IP}(\text{CF}_3)$ as 9.04 ± 0.5 or 9.03 ± 0.02 eV, respectively. However, an even more reliable value is possibly obtained by using the recent critically evaluated enthalpies $\Delta H_{f0}(\text{CF}_3\text{Br})$ and $\Delta H_{f0}(\text{CF}_3)$.¹ It may be noted that these enthalpies are not wholly independent of a previous determination of $\text{IP}(\text{CF}_3)$, but that this value 9.055 ± 0.011^3 is in any case in good agreement with our independent estimates above. Hence, with these enthalpies, we calculate $\Delta H_{f0}(\text{CF}_3^+) = 97.81 \pm 0.7$ kcal mol⁻¹ and $\text{IP}(\text{CF}_3) = 9.04 \pm 0.04$ eV as our preferred results.

Comparison with the other ionization energies listed in Table 1 shows that this result strongly supports the number of other investigations, experimental and theoretical, favoring an adiabatic IE between 9.05 and 9.10 eV. This emerging consensus has been identified and discussed by Irikura,⁵ who also offers an explanation why the lower IP deduced from ion–molecule reaction data may be erroneous. This leaves two other experimental studies which indicate a significantly lower IP. That of Jarvis and Tuckett⁴ proposes 8.8 ± 0.2 eV as an upper limit, with the authors favoring an actual value nearer to 8.6 eV. But because of the large error quoted, at the upper end of the range it approaches our current value. Aside from experimental error, this result, obtained from the $\text{CF}_3^+/\text{C}_3\text{F}_8$ AE, may also suffer from an uncertain $\Delta H_f(\text{C}_2\text{F}_5)$, and Irikura demonstrates how an alternative choice for this value could have raised the IP estimate to 8.98 ± 0.15 eV,⁵ which then does encompass our present value.

This then leaves the value 8.6 eV deduced from what now appears (see Table 2) to be an anomalously low CF_3^+ AE found in the molecular beam experiment of Clay et al.⁷ We thus consider the discrepancy between that study and our current one. Examining their ion yield curve visually, one sees that an extrapolation of their data with some kernel function, as here, would lead to a similar threshold value of ~ 12 eV, but that below that photon energy there is then a very weak, very extended tail leading to a quoted first onset several tenths of an electronvolt lower. We comment above on how the observed

onset AEs may be reduced by clustering of neutrals in the molecular beam and that such first onsets may not in fact correspond to AE_{0K} in very cold beams.

Contrasting with our observations, Clay et al. do report the detection of the stable dimeric (CF₃Br)₂⁺ ion in their experiments; it was inferred to result from ionization of both dimer and higher *n*-mer clusters of neutral CF₃Br. Unlike the present experiments seeded in He, these data were obtained from sample beams seeded in O₂ and Ar. One could expect these expansion conditions to foster a more extensive clustering of the neutral CF₃Br molecules. Since we do *not* observe stable (CF₃Br)₂⁺ ions, there is a possibility that the (CF₃Br)₂⁺ recorded by Clay et al. stems only from higher clusters, stabilized by evaporation. Consequently, one explanation for their lower observed onset may be the occurrence of more extensive clustering in their molecular beam source.

But the major probability is that the very weak onset in fact stems from a residual contribution of ionization by second-order light. It is evident from the uncorrected CF₂Br⁺ and CF₂⁺ yield curves presented by Clay et al. that at *hν* ≈ 12 eV and below these authors had substantial amounts of second-order light from their grating.⁷ Also it is known that photoionization of CF₃Br at 24 eV produces a significant amount of CF₃⁺ ion.¹⁶ Although the relevant CF₃⁺ ion yield curves of Clay et al. were stated to be corrected by some (unspecified) subtraction procedure, an incomplete correction could have resulted in some residual weak CF₃⁺ signal. In our experiment, we have demonstrated through the insertion of a LiF filter that the *only* source of CF₃⁺ in the 11.5–11.8 eV region is due to second-order light, and have eliminated this source of error in our ion yield data by the use of low-energy electron–ion coincidence data recording and the use of a high-order gas absorption filter.

V. Conclusions

Consistent estimates of the 0 K threshold for CF₃⁺ formation from CF₃Br were obtained from photoion yield data using the extrapolation procedure of Asher and Ruscic.^{3,15} The appearance of a thermal tail below this AE_{0K} was successfully rationalized by an examination of the characteristics of the molecular beam source, and special measurements were taken to eliminate other contributions to the tail caused by higher energy second-order light from the grating.

Our derived value for the CF₃ ionization energy of 9.04 ± 0.04 eV is in excellent agreement with recent calculations, and a strong experimental consensus is now also emerging in favor of this being the correct adiabatic ionization potential. The present value also serves to corroborate those other experimental determinations placing the ionization energy of CF₃ around 9.05 eV. While there exist experimental determinations placing this IP up to 0.5 eV lower in energy, convincing arguments can now be advanced as to why these determinations may be erroneous.

Acknowledgment. We thank the staff of LURE for their technical support of this experiment and are particularly indebted

to M. Vervloet and L. Nahon for assistance with the use of beamlines SA63 and SU5, respectively. Access to LURE was supported by the Commission of the European Union. Several helpful comments were made by T. Baer, and we acknowledge a referee who pointed out the significance of using CF₃–Br bond energies directly to obtain IP estimates which are fully independent of previous determinations of the CF₃ IP. Finally, we thank R. Tuckett for drawing the CF₃ ionization energy problem to our attention, for continuing helpful discussions on the topic, and for providing the unpublished CF₃Br TPES to corroborate our own observations.

References and Notes

- (1) Ruscic, B.; Michael, J. V.; Redfern, P. C.; Curtiss, L. A.; Raghavachari, K. *J. Phys. Chem. A* **1998**, *102*, 10889.
- (2) Lifshitz, C.; Chupka, W. A. *J. Chem. Phys.* **1967**, *47*, 3439.
- (3) Asher, R. L.; Ruscic, B. *J. Chem. Phys.* **1997**, *106*, 210.
- (4) Jarvis, G. K.; Tuckett, R. P. *Chem. Phys. Lett.* **1998**, *295*, 145.
- (5) Irikura, K. K. *J. Am. Chem. Soc.* **1999**, *121*, 7689.
- (6) Horn, M.; Oswald, M.; Oswald, R.; Botschwina, P. *Ber. Bunsen-Ges. Phys. Chem.* **1995**, *99*, 323.
- (7) Clay, J. T.; Walters, E. A.; Grover, J. R.; Willcox, M. V. *J. Chem. Phys.* **1994**, *101*, 2069.
- (8) Walter, T. A.; Lifshitz, C.; Chupka, W. A.; Berkowitz, J. J. *J. Chem. Phys.* **1969**, *51*, 3531.
- (9) Dyke, J. M.; Lewis, A. E.; Morris, A. *J. Chem. Phys.* **1984**, *80*, 1382.
- (10) Tichy, M.; Jahavery, G.; Twiddy, N. D.; Ferguson, E. E. *Int. J. Mass Spec. Ion Proc.* **1987**, *79*, 231.
- (11) Fisher, E. R.; Armentrout, P. B. *Int. J. Mass Spec. Ion Proc.* **1990**, *90*, R1.
- (12) Dixon, D. A.; Feller, D.; Sandrone, G. *J. Phys. Chem. A* **1999**, *103*, 4744.
- (13) Ricca, A. *J. Phys. Chem. A* **1999**, *103*, 1876.
- (14) Botschwina, P.; Horn, M.; Oswald, R.; Schmatz, S. *J. Elec. Spec. Relat. Phenom.* **2000**, *108*, 109.
- (15) Asher, R. L.; Appleman, E. H.; Ruscic, B. *J. Chem. Phys.* **1996**, *105*, 9781.
- (16) Creasey, J. C.; Smith, D. M.; Tuckett, R. P.; Yoxall, K. R.; Codling, K.; Hatherly, P. A. *J. Phys. Chem.* **1996**, *100*, 4350.
- (17) Richard-Viard, M.; Delboulbe, A.; Vervloet, M. *Chem. Phys.* **1996**, *209*, 159.
- (18) Nahon, L.; Alcaraz, C.; Marlats, J. L.; Lagarde, B.; Polack, F.; Thissen, R.; Lepère, D.; Ito, K. *Rev. Sci. Instr.* **2001**, *72*, 1320.
- (19) Mercier, B.; Compin, M.; Prevost, C.; Bellec, G.; Thissen, R.; Dutuit, O.; Nahon, L. *J. Vac. Sci. Technol. A* **2000**, *18*, 2533.
- (20) Powis, I.; Dutuit, O.; Richard-Viard, M.; Guyon, P.-M. *J. Chem. Phys.* **1990**, *92*, 1643.
- (21) Cvitas, T.; Güsten, H.; Klasinc, L.; Novadj, I.; Vancik, H. *Z. Naturfor. A* **1978**, *33*, 1528.
- (22) Weitzel, K. M.; Booze, J. A.; Baer, T. *Chem. Phys.* **1991**, *150*, 263.
- (23) Booze, J. A.; Baer, T. *J. Chem. Phys.* **1992**, *96*, 5541.
- (24) Powis, I. *Mol. Phys.* **1980**, *39*, 311.
- (25) Lane, I. C.; Powis, I. *J. Phys. Chem.* **1993**, *97*, 5803.
- (26) Wheatley, R. J., personal communication, 1999.
- (27) Weitzel, K. M.; Booze, J. A.; Baer, T. *Z. Phys. D* **1991**, *18*, 383.
- (28) Tsang, W. *J. Phys. Chem.* **1986**, *90*, 414.
- (29) Skorobogatov, G. A.; Dymov, B. P.; Nedozeleva, I. V. *Zh. Obshch. Khim.* **1996**, *66*, 1824.
- (30) Dymov, B. P.; Skorobogatov, G. A.; Khripun, V. K. *Zh. Fiz. Khim.* **1991**, *65*, 2085.